

All-electron theory of the coupling between laser-induced coherent phonons in bismuth

Euwe S. Zijlstra,* Larisa L. Tatarinova, and Martin E. Garcia
Theoretische Physik, Universität Kassel, Heinrich-Plett-Str. 40, 34132 Kassel, Germany
 (Dated: August 15, 2018)

Using *first principles*, all-electron calculations and dynamical simulations we study the behavior of the A_{1g} and E_g coherent phonons induced in Bi by intense laser pulses. We determine the potential landscapes in the laser heated material and show that they exhibit phonon-softening, phonon-phonon coupling, and anharmonicities. As a consequence the E_g mode modulates the A_{1g} oscillations and higher harmonics of both modes appear, which explains recent isotropic reflectivity measurements. Our results offer a unified description of the different experimental observations performed so far on bismuth.

PACS numbers: 78.70.-g,63.20.Kr,71.15.Pd,63.20.Ry

Intense femtosecond laser pulses can induce a nonequilibrium state which leads to sudden and dramatic changes in the potential energy surfaces of different solids [1]. This property can be used to excite and manipulate coherent lattice vibrations, as has been recently shown by several experiments [2, 3, 4, 5] and simulations [6]. In the last years, a variety of experiments on laser excitation of coherent phonons has been performed on bismuth [7, 8, 9, 10], which is a particularly interesting solid since its ground-state structure exhibits a Peierls distortion. From the different studies done so far, a number of fundamental aspects still remain unexplained, like the detection of higher harmonics [9] and the appearance of modes that are forbidden by symmetry in isotropic reflectivity measurements [8].

In this letter we perform *ab initio* calculations which show, for the first time, the existence of a coupling between laser-induced phonon modes of different symmetry. In addition, we demonstrate that the large amplitude atomic vibrations excited by femtosecond laser pulses are affected by the anharmonic part of the potential energy surface, which creates overtones.

The structure of Bi can be derived from a simple cubic atomic packing in two steps. First a simple cubic lattice is deformed by elongating it along one of the body diagonals, which is indicated by a thin line in Fig. 1. A Peierls instability

then causes the atoms to be displaced along the same diagonal, in opposite directions (Fig. 1). The magnitude of the displacements is determined by the detailed interaction between the Bi nuclei and the electrons. When the electrons are heated with a laser, the equilibrium positions of the atoms change. If the duration of the laser pulse is short in comparison with the timescale of the atomic motion, the ions are lifted at their original equilibrium positions to the potential energy surface that is created by the hot electrons, from where they start to swing about their new equilibrium positions [2]. This motion of the atoms corresponds to the coherent excitation of the dispersive A_{1g} phonons (Fig. 1). Coherent E_g phonons, which correspond to the motion of the atoms in the plane perpendicular to the elongated body diagonal, are also excited by a laser, through Raman scattering [4]. In Bi the existence of laser-excited coherent E_g phonons has been demonstrated through electro-optical measurements [11].

Recent experiments have shown three exciting results: (i) Through a measurement of the geometrical structure factors of two x-ray diffraction peaks the most accurate value so far of the maximal displacement of the atoms due to the interaction with a short laser pulse has been determined [7]. (ii) In isotropic reflectivity measurements apart from the softened A_{1g} phonon mode (2.52 THz) a signal at lower frequency (1.61 THz) that can be attributed to the E_g phonons has been detected [8]. In addition there is also a peak at 3.44 THz [12]. (iii) In another study higher harmonics of the softened A_{1g} phonon frequency have been detected [9].

It is the aim of this letter to provide a theoretical explanation of these experimental results. To achieve this we performed a dynamical simulation for the E_g and A_{1g} degrees of freedom. The potential energy surface on which the atoms moved was calculated with the all-electron full-potential linearized augmented plane wave (LAPW) computer program WIEN2k [13], which is based on density functional theory (DFT).

For our ground state DFT calculations we used the experimental unit cell parameters of Bi (spacegroup R3m, $a = 4.5332 \text{ \AA}$, $c = 11.7967 \text{ \AA}$). The Bi atoms occupied the 6c sites (0,0, z), where z gives the position of the atoms along the above-mentioned diagonal. We performed DFT calculations for $z = 0.230, 0.231, \dots, 0.250 c$, where $z = 0.250 c$ represents the structure in the absence of the atomic displacement

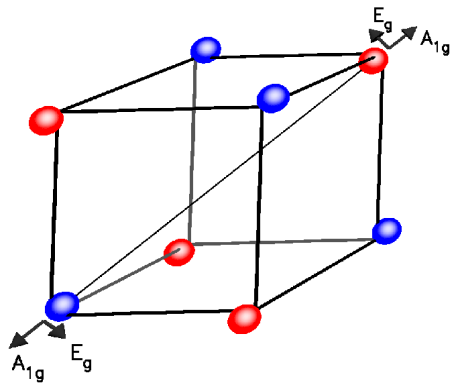


FIG. 1: (Color online) Structure of Bi (see text). In the A_{1g} phonon mode the atoms move in the direction of the thin line as indicated for two atoms (long arrows). In the E_g phonon modes the atoms move in the perpendicular plane (e.g., in the directions of the short arrows).

due to the Peierls instability and $z = 0.234 c$ is the experimental equilibrium structure. Based on the total energies for these z we could perform a simulation of the coherent A_{1g} phonons. The degrees of freedom corresponding to the E_g phonons (x and y) were taken into account by varying $x = 0.000, 0.001, \dots, 0.010 a$ and $z = 0.234, 0.235, \dots, 0.250 c$. The potential energy surface, on which the ions moved, was then fitted to the function

$$E_{\text{tot}} = \sum_{p=0}^4 a_p (z - 0.25)^{2p} + (x^2 + y^2) \sum_{p=0}^2 b_p (z - 0.25)^{2p}, \quad (1)$$

where the last term describes a coupling between the motion in the z and the x (y) directions. The fact that it is proportional to $(x^2 + y^2)$ can be easily understood from the symmetry of the crystal structure, since the coupling cannot depend on the sign of the displacement (see Fig. 1). Other important details of our DFT calculations were as follows. LAPW's with energies up to 12.0 Ry were included in the basis. Inside the atomic spheres (with radii of 1.376 Å) additional $5d$, $6s$, $6p$, and $6d$ local orbitals were used. Spin-orbit coupling was treated in a second variational procedure, where the scalar relativistic eigenstates up to 3.0 Ry and local $6p_{1/2}$ orbitals were used as a basis for the relativistic calculation. The entire Brillouin zone was sampled with 512 k points using temperature smearing ($T_e = 1$ mRy).

At elevated temperatures we assumed that there was no exchange of heat between the electrons and the ions. As a consequence the entropy of the electrons was a constant of motion [14]. We further assumed that the electrons were perfectly thermalized at all times due to electron-electron interactions. Therefore the occupation numbers of the Kohn-Sham states were always given by a Fermi-Dirac distribution. Recently, another approach has been proposed [10, 15, 16], where the occupation numbers for the electrons and holes of laser-excited Te [15, 16] and Bi [10] are modeled with two temperature distributions using different chemical potentials for the electrons and the holes while keeping the number of electron-hole pairs constant. Although this so-called two-chemical-potential model might work well for semiconductors we do not believe that it is appropriate for Bi at high laser fluences as we discuss below.

To compare the predictions of the two-chemical-potential model and the model where the constant entropy of the electrons was the only constraint we performed additional calculations assuming two chemical potentials. In agreement with [10] we chose the electron and hole temperatures $T_e = T_h = 0.5$ eV at $z = 0.234 c$. No heat was assumed to be exchanged between the electrons or the holes and the ions. Therefore the entropy of the electrons and holes were constants of motion. In this respect we did not follow the method of [10, 15, 16], where the temperatures of the electrons and the holes have been kept constant, while the atoms moved on the total energy surface, because it yields incorrect forces [17].

The potential energy surface $E_{\text{tot}}(T_e)$ on which the ions moved at elevated electronic temperatures was calculated

from

$$E_{\text{tot}}(T_e) = E_{\text{tot}}(\text{gs}) + \Delta E_{\text{band}}, \quad (2)$$

where $E_{\text{tot}}(\text{gs})$ was the self-consistent total energy of the electronic ground state and $\Delta E_{\text{band}} = E_{\text{band}}(T_e) - E_{\text{band}}(\text{gs})$. This approach is based on the interpretation of the Kohn-Sham energies as single-electron excitation energies. In standard temperature-dependent DFT the electronic occupation numbers are incorporated in the self-consistent cycle to take into account possible screening effects. We also performed such standard temperature-dependent DFT calculations and found that the differences between the predictions of both approaches were very small (the main effect was that the electronic entropies in both approaches had to be scaled). For this reason and also because it is not clear that the self-consistent approach always leads to better results we used the computationally less time-consuming non-self-consistent treatment of Eq. (2). Our results for different laser-induced initial electronic temperatures are summarized in table I.

In the electronic ground state the total energy E_{tot} was minimized for $z = 0.2346 c$. At this parameter the A_{1g} and E_g phonon frequencies were 2.89 and 1.94 THz, respectively, in reasonable agreement with experiment [$z = 0.2341 c$, $\nu(A_{1g}) = 2.92$, and $\nu(E_g) = 2.16$ THz] [8] and with earlier calculations [$z = 0.2336 c$, $\nu(A_{1g}) = 2.93$ THz] [10]. The differences with the experimental results are probably due to the local density approximation [18], which we used for the exchange and correlation energy. The differences with the earlier calculations [10] are probably due to the Bi pseudopotential used in those calculations. The present all-electron calculations do not rely on a pseudopotential and should be more accurate.

In the excited electronic states (table I) the potential energy surfaces are flatter than the ground state potential energy surface (Fig. 2). As a consequence the phonon frequencies are lower. For large amplitude coherent phonons anharmonicity may further lower the phonon frequencies [8]. As mentioned above, in [7] the maximal laser-induced displacement Δz has been accurately determined: Under the influence of a laser pulse that leads to a softening of the A_{1g} frequency from 2.92 to 2.12 THz, $\Delta z = 0.0085 \pm 0.0021 c$. For the electronic entropy $S_e = 0.428 k_B/\text{atom}$ we reproduced this softening of the A_{1g} phonon frequency. According to our calculations 16% of the decrease of the A_{1g} phonon frequency was due to the anharmonicity of the potential (The harmonic frequency was 2.24 THz). Our value for the amplitude of the A_{1g} motion was $\Delta z = 0.0075 c$, in agreement with the experimental value [7].

After the initial softening of the A_{1g} phonons, the frequency returns to its original value within roughly 10 ps [8]. We discuss the origin of this frequency hardening by comparing our results and the experimental results of [8], where the A_{1g} phonon frequency has been resolved in time. For the electronic entropy $S_e = 0.300 k_B/\text{atom}$ ($T_e = 17.6$ mRy at $z = 0.234 c$) our calculated A_{1g} phonon frequency was 2.45 THz, the initial A_{1g} frequency obtained in [8]. After 0.3 ps

TABLE I: Coefficients for the potential energy surfaces of Eq. (1) as a function of the electronic entropy S_e . In Eq. (1) E_{tot} is given in mRy / atom, x and y are given in units of the lattice parameter a , and z is given in units of c . The electronic temperature T_e and the number of electron-hole pairs N_{e-h} (expressed in % of the valence electrons), which are not constants of motion, are given for $z = 0.234 c$.

S_e (k_B / atom)	T_e (mRy)	N_{e-h} (%)	a_0	a_1 (10^4)	a_2 (10^8)	a_3 (10^{11})	a_4 (10^{14})	b_0 (10^3)	b_1 (10^7)	b_2 (10^{10})
0.164	12.7	0.50	-12.087	-3.0663	1.2609	-2.1728	1.7787	-3.35	4.202	-7.48
0.260	16.2	0.81	-11.428	-2.4474	1.0267	-1.6487	1.3035	-2.52	3.360	-5.30
0.300	17.6	0.95	-11.039	-2.2087	0.9417	-1.4619	1.1342	-2.21	3.070	-4.58
0.428	21.9	1.41	-9.392	-1.5468	0.7313	-1.0278	0.7519	-1.36	2.392	-2.99
0.431	22	1.42	-9.346	-1.5328	0.7272	-1.0200	0.7452	-1.34	2.380	-2.96

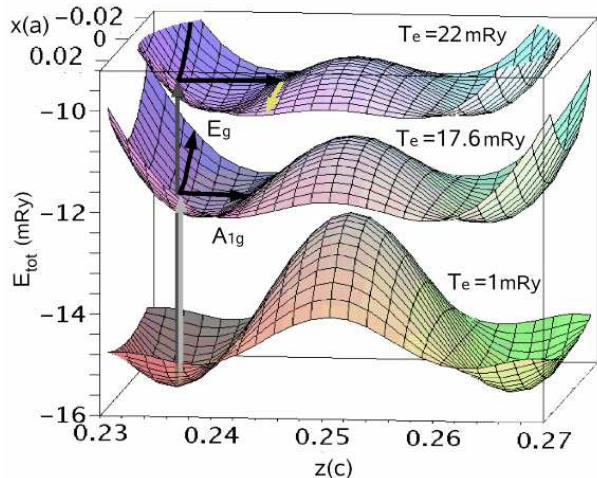


FIG. 2: (Color online) Potential energy surfaces for the ground state ($T_e = 1$ mRy) and for excited electronic states ($T_e = 17.6$ and 22 mRy at $z = 0.234 c$). Vertical arrows show transitions of the atoms from the ground state to an excited energy surface. The A_{1g} and E_g phonon modes are indicated. On the surface labeled $T_e = 22$ mRy the curvature in the x direction becomes negative when the atoms are at their maximal displacement in the z direction. This negative curvature is indicated by a light (yellow online) arrow.

the A_{1g} frequency in [8] increased to 2.52 THz. Our results indicated that at most 0.03 THz of this increase can be explained by the anharmonicity of the potential energy surface (The harmonic frequency was 2.48 THz), in agreement with experiments using two time-delayed pump laser pulses [10] that have shown that the frequency of the A_{1g} phonon mode averaged over five periods is the same within 1% independent of the amplitude of the oscillations for frequencies as low as 2.65 THz. Note however that anharmonicity plays a substantial role in the phonon softening in [7] as discussed above. Instead a decrease of the electronic entropy to $S_e = 0.260 k_B/\text{atom}$ yielding an A_{1g} frequency of 2.52 THz is probably responsible for the frequency increase observed in [8]. The accompanying decrease in the number of electron-hole pairs by 15% (calculated at $z = 0.234 c$) corresponds to a decay time of 1.8 ps, which agrees well with the experimentally determined electronic background decay time of 1.78 ± 0.08 ps, which is independent of the laser fluence [19]. The loss of entropy of the electrons near the surface is most likely due to

diffusion of hot electrons away from the surface region (the penetration depth of the laser $d \approx 17$ nm) and may also be partly due to the exchange of heat of the electrons with the ions via electron-phonon coupling, two processes that were not explicitly taken into account in our calculations.

At this point it is necessary to discuss the limitations of the two-chemical potential model proposed in [15]. According to [20] the electron-hole recombination time in Bi at 300 K is about 1 ps. In a highly excited electronic state this time is expected to be considerably shorter. So within less than four phonon periods the electrons and the holes obtain a common chemical potential. To check the validity of the two-chemical-potential model we applied it and found that the chemical potential of the holes was greater than the chemical potential of the electrons, which means that upon reaching a common chemical potential the number of electron-hole pairs would increase, which would then give rise to a substantial further lowering of the phonon frequencies (we estimated that the ions would even go over the barrier at $z = 0.25 c$), in contradiction with experiment [8]. Therefore, we believe that the two-chemical potential model [10] does not provide a realistic description of the electron dynamics in Bi. We can however not exclude that this model might be appropriate for semiconductors or for Bi at lower laser fluences.

We now consider the coupling between the A_{1g} and the E_g phonons. Figures 3(a) and 3(b) show the intensity of the Fourier transform of the z coordinate of the atoms. Higher harmonics of the main A_{1g} peak at 2.52 THz, which have also been observed experimentally [9], and which are a consequence of the anharmonicity of the potential, are indicated. For the initial velocity of the atoms in the x direction (coherent E_g phonons) we chose a value that gave a peak to peak amplitude $\Delta x = 0.4\Delta z$, in agreement with [21]. In Fig. 3(b) it is clear from the peaks that there is a considerable coupling between the A_{1g} and E_g phonons. In Eq. (1) the A_{1g} phonon mode couples to $x^2 + y^2$, a signal with double the E_g frequency, $2\nu(E_g)$. Accordingly an analysis of the x coordinate of the atoms showed that the frequency of the highest peak induced by the phonon-phonon coupling, labeled $2E_g$ in Fig. 3(b), (3.32 THz) equaled $2\nu(E_g)$. Experimentally this peak has been observed at 3.44 THz [12]. So in our calculations $\nu(E_g)$ was slightly lower than in the experiment [12], which is consistent with our ground state calculation. The frequency

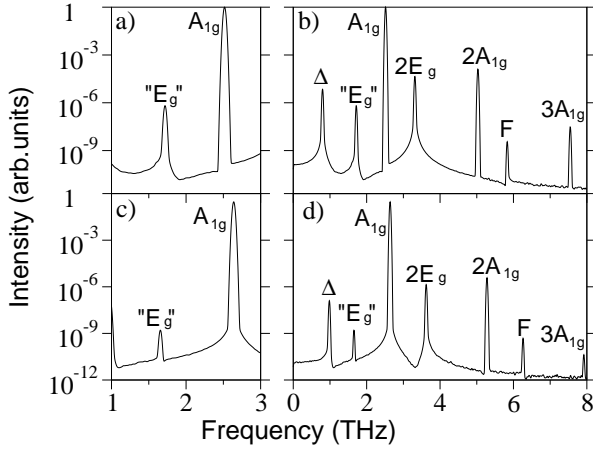


FIG. 3: Fourier transforms (intensities) of the z coordinate of the atoms for two different simulations: a), b) $T_e = 16.2$ and c), d) $T_e = 12.7$ mRy at $z = 0.234 c$. All curves have been convoluted with a Gaussian with a full width at half maximum of 0.03 THz. The left panels a) and c) show that the height of the peak labeled “ E_g ” depends very sensitively on the laser fluence, which was twice lower in c) than in a). Experimentally this has been shown in [8].

of the peak labeled “ E_g ” in Fig. 3(b) (1.72 THz) is given by $2\nu(A_{1g}) - 2\nu(E_g)$. Experimentally this peak has been observed at 1.61 THz [8]. Our value was slightly higher than in the experiment [8] because the calculated $\nu(E_g)$ was slightly lower. Note that in [8] this peak has been identified with the E_g mode. However, since there is no coupling term linear in x (y), and since the E_g mode produces modulations of the A_{1g} oscillations, it is clear that no peak of the power spectrum can have the frequency $\nu(E_g)$, whereas the difference $2\nu(A_{1g}) - 2\nu(E_g)$ should be present. The fact that the “ E_g ” peak has an intensity of only $I(“E_g”) = 7 \cdot 10^{-7} I(A_{1g})$ and that it has nevertheless been observed experimentally [8] indicates that the laser-induced amplitude of the E_g mode is probably larger than $\Delta x = 0.4\Delta z$, which we used in our simulation. According to [21] the relative Raman cross sections of the A_{1g} and E_g modes are indeed temperature dependent. The sensitivity of the results to the initial conditions is further underlined by a calculation with $\Delta x = 1.2\Delta z$, for which we found $I(“E_g”) = 3 \cdot 10^{-4} I(A_{1g})$. Finally, we note that the peak labeled Δ in Fig. 3(b) [$0.80 \text{ THz} = 2\nu(E_g) - \nu(A_{1g})$] is experimentally hard to observe because of broadened spectral structures near zero frequency [12]. Similarly the peak labeled F in Fig. 3(b) [$2\nu(E_g) + \nu(A_{1g})$] probably has too low an intensity to be observed.

Figures 3(c) and 3(d) were calculated for the case where the energy absorbed from the laser was twice as small as in Figs. 3(a) and 3(b) ($T_e = 12.7$ mRy at $z = 0.234 c$). It shows that the intensity of the peak “ E_g ” became orders of magnitude lower upon reducing the laser fluence by a factor of two.

Therefore a strong laser pulse is needed to observe the A_{1g} - E_g phonon coupling, which has also been found experimentally in [8].

Another interesting result that we found is that the coupling between the A_{1g} and E_g modes became very strong for $S_e \gtrsim 0.431 k_B/\text{atom}$ ($T_e = 22$ mRy at $z = 0.234 c$): In this case the curvature of the potential energy surface in the x direction became negative every time z reached its maximum value (Fig. 2). We found that the amplitude of the E_g mode increased exponentially even when the initial velocity in the x direction was very small.

In conclusion, we presented a dynamical simulation of coherent laser-induced A_{1g} and E_g phonons in Bi on a potential energy surface that was obtained by all-electron, *first principles* calculations. Using these simulations we could explain the effects of anharmonicity and A_{1g} - E_g phonon coupling that take place after the interaction with ultrashort, intense laser pulses. We found good agreement with all experiments performed so far [7, 8, 9, 10, 11, 12].

This work has been supported by the Deutsche Forschungsgemeinschaft (DFG) through the priority program SPP 1134 and by the European Community Research Training Network FLASH (MRTN-CT-2003- 503641).

* zijlstra@physik.uni-kassel.de

- [1] P. Stampfli and K. H. Bennemann, Phys. Rev. B **49**, 7299 (1994).
- [2] H. J. Zeiger et al., Phys. Rev. B **45**, 768 (1992).
- [3] M. Hase et al., Nature (London) **426**, 51 (2003).
- [4] G. A. Garrett et al., Phys. Rev. Lett. **77**, 3661 (1996).
- [5] M. Bargheer et al., Science **306**, 1771 (2004).
- [6] T. Dumitrica et al., Phys. Rev. Lett. **92**, 117401 (2004).
- [7] K. Sokolowski-Tinten et al., Nature **422**, 287 (2003).
- [8] M. Hase et al., Phys. Rev. Lett. **88**, 067401 (2002).
- [9] O. V. Misochko, M. Hase, and M. Kitajima, JETP Lett. **78**, 75 (2003).
- [10] É. D. Murray et al., Phys. Rev. B **72**, 060301(R) (2005).
- [11] M. Hase et al., Appl. Phys. Lett. **69**, 2474 (1996).
- [12] M. Hase, (private communication).
- [13] P. Blaha et al., *WIEN2k, An Augmented Plane Wave + Local Orbitals Program for Calculating Crystal Properties* (Karlheinz Schwarz, Techn. Universität Wien, Austria, 2001).
- [14] P. Stampfli and K. H. Bennemann, Phys. Rev. B **42**, 7163 (1990).
- [15] P. Tangney and S. Fahy, Phys. Rev. Lett. **82**, 4340 (1999).
- [16] P. Tangney and S. Fahy, Phys. Rev. B **65**, 054302 (2002).
- [17] R. M. Wentzcovitch, J. L. Martins, and P. B. Allen, Phys. Rev. B **45**, 11372(R) (1992).
- [18] J. P. Perdew and Y. Wang, Phys. Rev. B **45**, 13244 (1992).
- [19] M. F. DeCamp et al., Phys. Rev. B **64**, 092301 (2001).
- [20] M. Hase et al., Phys. Rev. Lett. **93**, 109702 (2004).
- [21] J. B. Renucci et al., Phys. Status Solidi **60**, 299 (1973).